# Investigation of the UV/Visible Absorption Spectra of Merocyanine Dyes Using Time-Dependent Density Functional Theory

**ARTICLE** *in* THE JOURNAL OF PHYSICAL CHEMISTRY A · JANUARY 2007

Impact Factor: 2.69 · DOI: 10.1021/jp064059p · Source: PubMed



**3 AUTHORS**, INCLUDING:

Maxime Guillaume
Solvay
**35** PUBLICATIONS **729** CITATIONS
SEE PROFILE

Benoît Champagne
University of Namur
**401** PUBLICATIONS **8,719** CITATIONS
SEE PROFILE

# Investigation of the UV/Visible Absorption Spectra of Merocyanine Dyes Using Time-Dependent Density Functional Theory

**Maxime Guillaume and Benoît Champagne***

*Laboratoire de Chimie Théorique Appliquée, Facultés Universitaires Notre-Dame de la Paix, rue de Bruxelles 61, B-5000 Namur, Belgium*

**Freddy Zutterman**

*Agfa-Gevaert N.V., Septestraat 27, B-2640 Mortsel, Belgium*

*Received: June 28, 2006; In Final Form: September 27, 2006*

The visible spectral properties of a set of merocyanine dyes have been determined experimentally and compared to theoretical estimates calculated using time-dependent density functional theory. Three families of merocyanines have been investigated. The merocyanines of the first class contain the 4-thiazolidinone, 2-thioxo group in resonance with different donor groups. In the second family, they present a common pyrrolo[2,3-*c*]pyrazole-6-(2*H*)-acetic acid, the 4-[4-(dialkylamino)phenyl]-3,5-dihydro-3,5-dioxo-2-phenyl group with different substituents on the two phenyl rings, while in the third family, they are constituted of an isoxazolone group linked via a conjugated polyenic segment to an aminophenyl group. Two hybrid exchange-correlation functionals have been used, whereas solvent effects have been included using the integral equation formalism of the polarizable continuum model. Moreover, for one compound, the vibrational structure of the electronic transitions has been determined by calculating the Franck−Condon factors within the Born−Oppenheimer approximation. The calculations show that the dominant transitions present a $\pi-\pi^*$ character. This approach reproduces nicely the variations of excitation energies with the nature of the merocyanine so that least-squares fits can be used to correct for the major systematic errors of the computational scheme and to reach an accuracy of 0.09 eV or better. Part of these systematic errors is shown to originate from the description of the solvent effects, whereas vibronic effects can account for most of the remaining differences.

## I. Introduction

Designing dyes and tuning their optical properties is of particular interest in many areas of the science, technology, and industry of colors,[1] for developing new display devices,[2] new inks and paints, new sensors, and detectors.[3,4] In these design processes, the tools of theoretical chemistry can be valuable, in particular, to deduce structure−property relationships, which can help to rationalize the design of dyes and to refine their structure in order to optimize their absorption color, solubility, and/or solid-state structure, depending on the type of applications for which they are needed.

The present work focuses on the excitation energies of a well-known class of dyes, the family of merocyanines. This kind of compound presents several typical optical properties, mainly because of the conjugated pathway between the donor and acceptor substituents. Among them, the nonlinear optical (NLO) properties have been of particular interest[5−7] while many experimental and theoretical works addressed their solvatochromism. Indeed, when changing the solvent, merocyanine dyes can exhibit bathochromic, hypsochromic, or even both types of shifts depending on their structure, which has fostered the interest for these compounds as solvent (polarity) sensors.[8]

Many of these studies on NLO and solvatochromism have been carried out at semiempirical levels of approximation, in combination with a method to take into account the interactions with the solvent or more generally the surroundings. These encompass (i) the solvaton conformations spectra-intermediate neglect of differential overlap (CS INDO) scheme of Baraldi et al.,[9,10] which takes into account the electrostatic interactions between the solvent and the solute, (ii) the atom superposition and electron delocalization molecular orbital (ASED-MO) method of Abdel-Halim and Awad,[11,12] and (iii) the self-consistent reaction field (SCRF) scheme associated with the PM3 semiempirical parametrization of Hamman and El-Nahas.[13] Moreover, Millié et al.[14] used a configuration interaction (CI) approach where the configurations are selected perturbatively (CIPSI). This approach was combined with a CS INDO Hamiltonian and was coupled with the Frenkel exciton theory to estimate the optical properties of organized assemblies of merocyanine dyes and the impact of the different environmental interactions. Besides these semiempirical approaches, Mach et al.[15] found a good correlation between the experimental and the theoretical optical properties of the merocyanine 540 by determining the geometrical structures using density functional theory (DFT) and evaluating the excitation energies at the configuration interaction singles (CIS) level. The vertical SCRF approach developed by Liu et al.[16] reproduced the solvatochromism of Brooker's merocyanine in different solvents. It is based on DFT calculations including both the surrounding solvent molecules and a polarizable continuum.

This broad range of studies and the various methodologies used so far to tackle the solvatochromism are representative of the importance and the need for adapted theoretical methods to evaluate the excitation energies while taking into account the solvent and the intermolecular interactions. This should help in predicting, explaining, and validating experimental spectroscopic

10.1021/jp064059p CCC: $33.50 
Published on Web 11/11/2006

data. Within this context, the scope of the present work consists of studying both experimentally and theoretically the UV/visible light absorption spectra in a series of compounds displaying a merocyanine-like structure, but differing by their molecular backbones and substituents.

The methodology to determine the excitation energies is the adiabatic approximation to the time-dependent density functional theory (TDDFT) approach.[17] This choice is motivated by the numerous illustrations of the validity of this scheme to determine the excitation energies of a broad range of organic and organometallic compounds[18−32] and by the difficulty to apply highly correlated approaches, such as coupled-cluster[33] or multireference[34] methods, on large molecular systems. Moreover, certain inherent errors of the TDDFT method have already been shown to be systematic, at least in a given family of molecules. These errors are mainly due to an incorrect description of the long-range character of the usual exchange-correlation functionals, leading to a poorer description of the charge transfer states and an inadequate description of the size effects.[35,36] Although promising solutions have appeared recently and would deserve a detailed investigation with respect to experimental data,[37−39] these drawbacks can be partially corrected by the application of a linear scaling approach, which has already been proved to remove these systematic errors, for instance, for NMR chemical shifts and excitations energies.[25,40] In this work, we follow this approach and propose an explanation for these limitations. The next section describes the theoretical and computational contexts. Then, section III presents and discusses the results, before conclusions are drawn in section IV.

## II. Experimental and Simulation Aspects

**II-1. Experimental Aspects.** Experimental absorption maxima were obtained from absorption spectra of very dilute solutions of the merocyanines in methanol, that is, solutions ranging between $10^{-5}$ and $10^{-4}$ mol/L. For this range of concentrations in methanol, the merocyanines investigated here do not form dimers or aggregates. The spectra were recorded at room temperature in a 1 cm cuvette on an Agilent 8453 UV/visible light spectrophotometer. To avoid saturation effects, the concentration was chosen such that the light absorption at the wavelength of maximum absorption was not higher than 90% of the incident beam intensity.

**II-2. Computational Aspects.** The geometry optimizations of the electronic ground state were carried out at the DFT level, with the hybrid B3LYP exchange-correlation functional and the split-valence 6-311G* basis set. The convergence criterion on the residual forces has been set to $1.5 \times 10^{-5}$ hartree/bohr or hartree/rad. The vertical excitation energies ($\Delta E$) have been calculated with the adiabatic approximation of the TDDFT using two hybrid exchange-correlation functionals, B3LYP and PBE0, including, respectively, 20 and 25% of the Hartree−Fock (HF) exchange. Two basis sets were employed in combination with the B3LYP functional, the 6-311G* and 6-311+G* basis sets, the last one including an additional set of diffuse s and p functions.

As discussed in the Introduction, one can expect important solvent effects on the optical properties. They are modeled using the integral equation formalism of the polarizable continuum model (IEFPCM).[41] This model represents the solvent as apparent charges spread over the surface of a cavity having the same shape as the solute. It takes into account the electrostatic interactions between these surface charges and the solute in a self-consistent manner. Furthermore, it enables us to account for the relaxation of the electronic structure upon excitation and for the influence of this relaxation on the charge distribution of the cavity. In this case of fast absorption processes, the inclusion of nuclear relaxations is avoided by employing a partitioning of the polarization vector in terms of fast electronic cloud reorganizations and slow solvent and solute nuclear motions.[42] These geometry optimizations and excitation energy calculations with or without the IEFPCM treatment were carried out using the Gaussian03 program package.[43]

The geometry relaxations in the excited states and the vibrational structures of the electronic transitions have also been addressed for one representative compound within the Born−Oppenheimer approximation by calculating the Franck−Condon factors. To account for these phenomena, often called vibronic effects, the first step consists of the geometry optimization of the excited states. Then, to determine the Franck−Condon factors, we evaluate the vibrational normal modes and frequencies for both the ground and the excited states. These calculations are performed with the TURBOMOLE program package,[44] which includes a recent analytical algorithm to determine the force constants of the excited states and thus their vibrational frequencies.[45] Following the study by Dierksen and Grimme,[46] the geometry optimizations and force constant calculations were carried out using the BHandHLYP exchange-correlation functional, containing 50% of the HF exchange, and the SV(P) basis set. Indeed, ref 46 shows that using an exchange-correlation functional with 50% of the HFexchange leads to a better agreement with experiment than using a pure density functional or a functional with 20% of the HF exchange (B3LYP). The Franck−Condon factors are then evaluated using the Doktorov and co-worker recursive expression,[47] according to the work of Spangenberg et al.[48]

## III. Results

**III-1. Structures and Geometries.** The molecular structures under investigation are sketched in Chart 1. They are classified according to their structure and denoted from **A** to **K**. The **A**−**E** molecules are characterized by a specific 4-thiazolidinone, 2-thioxo group in resonance with different donor groups. The **F**−**I** molecules present a common pyrrolo[2,3-*c*]pyrazole-6-(2*H*)-acetic acid, 4-[4-(dialkylamino)phenyl]-3,5-dihydro-3,5-dioxo-2-phenyl group while the substituents of the two phenyl rings vary. Molecules **J** and **K** are constituted of an isoxazolone group linked via a conjugated polyenic segment to an aminophenyl group bearing different substituents.

For the **B**−**E**, **J**, and **K** merocyanines, rotations around C−C double bonds can lead to different stable conformers. Their major geometrical characteristics and relative energies listed in Table 1 demonstrate that in a few cases several conformers have to be considered at 298.15 K. This is accounted for in our simulation by using the Maxwell−Boltzmann distribution. The interaction between the methyl group on the N atom and the CO group in compound **B** favors the conformer with $\theta_{SCCS} = \pi$. In compound **C**, the ethyl substituent on N leads to a thermodynamic preference for the conformer with $\theta_{NCCC} \sim \pi$, whereas the methyl group in compound **D** is associated with the reverse stability ordering since the conformer with $\theta_{NCCC} \sim 0$ is the most stable. Nevertheless, for both **C** and **D** compounds, the second most stable conformer presents a non-negligible weight (10−20%) when using Maxwell−Boltzmann averaging. On the other hand, the presence of a methyl group on one of the inner C atoms of the conjugated linker in compound **E** favors one conformer and reduces considerably the weight of the others.

**III-2. Nature of the Dominant Electronic Excitations.** The experimental spectra are characterized by a dominant low-energy

**CHART 1: Structure and Labelling of the Merocyanine Dyes**[a]

**A.**

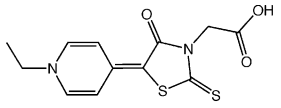

**B.**

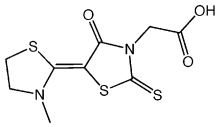

**C.**

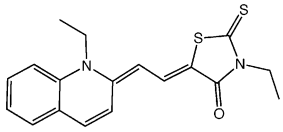

**D.**

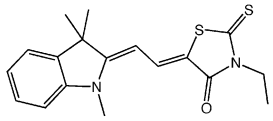

**E.**

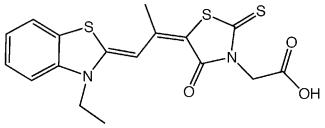

**F.**

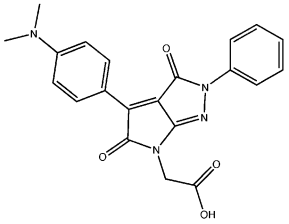

**G.**

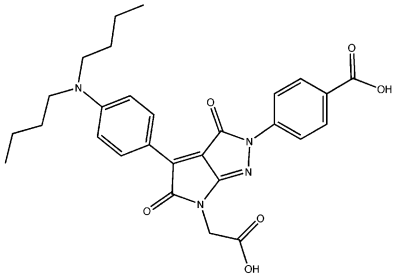

**H.**

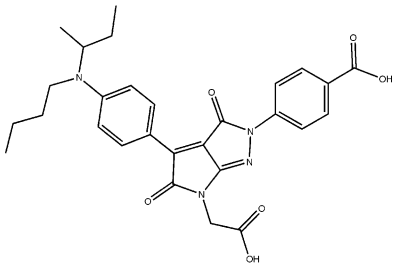

**I.**

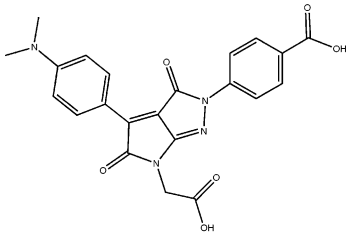

**J.**

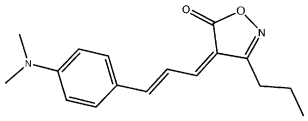

**K.**

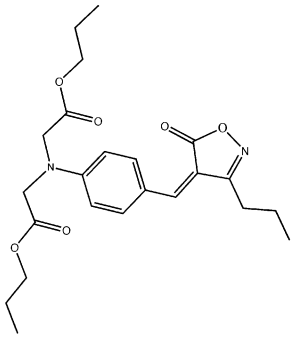

[a] The most stable conformer of each compound is represented as determined according to Table 1.

absorption band. The calculations performed at the different TDDFT levels of approximation also indicate the presence of one dominant transition, the other ones having oscillator strengths one to two orders of magnitude smaller. Therefore, the following discussion will focus of this transition since it governs the optical properties of the dyes. For all systems, it corresponds to the first dipole-allowed $\pi-\pi^*$ transition of which the dominant configurations involve the HOMO and/or HOMO $-$ 1 with the LUMO and/or LUMO $+$ 1. The sketches of these molecular orbitals are given in Figure 1 for one representative molecule of each series, the **B**, **F**, and **J** molecules. For molecule **B** the first excitation is typically a $\pi-\pi^*$ transition involving the central C$-$C double bond. For molecule **F**, the excitation involves the electron displacement from the two external phenyl rings to the central moiety. Then, for molecule **J**, the transition goes from the phenylamino group to the isoxazolone moiety and is accompanied by a $\pi-\pi^*$ transition in the polyenic segment. Thus, only valence $\pi/\pi^*$ molecular orbitals are involved in the electronic transition.

**III-3. Effect of the Method of Calculation.** Table 2 lists the excitation energies calculated at different levels of approximation, including Maxwell$-$Boltzmann averaging when more than one conformer has a non-negligible weight at 298.15 K. Indeed, a similar procedure was recently shown to be necessary in order to account for structural effects on the UV/visible light absorption spectra of benzimidazolo[2,3-*b*]oxazolidines.[49] It can be observed that, in all cases, adding diffuse functions, when using the B3LYP functional, leads to a small decrease of the excitation energies, from 0.03 eV (compounds **C**, **E**, and **K**) to 0.07 eV (compound **A**). This is consistent with the character of the transitions that mainly implies valence molecular orbitals. On the other hand, using the PBE0 functional leads to a small increase of the excitation energies, ranging from 0.06 to 0.09 eV. These differences of excitation energies between the methods are small with respect to the amplitude

**TABLE 1: B3LYP/6-311G* Optimized Torsion Angles (deg) and Relative Energies (kcal/mol) of the Important Conformers of the Merocyanines B−E, J, and K**

| | conformer no. | $\Delta E$ (kcal/mol) | torsion angle no. 1[a] | torsion angle no. 2[b] |
|---|---|---|---|---|
| **B** | 1 | 0.00 | 180.0 | |
| | 2 | 2.52 | −8.4 | |
| **C** | 1 | 0.00 | 0.1 | −175.0 |
| | 2 | 0.89 | −179.6 | −175.1 |
| | 3 | 3.63 | 2.4 | 11.4 |
| | 4 | 5.97 | −177.7 | 11.9 |
| **D** | 1 | 0.00 | 0.1 | 0.2 |
| | 2 | 1.33 | 0.1 | −179.8 |
| | 3 | 1.98 | 179.7 | −0.2 |
| | 4 | 2.90 | 179.9 | −189.9 |
| **E** | 1 | 0.00 | 179.4 | 177.1 |
| | 2 | 5.26 | −5.5 | −19.9 |
| | 3 | 7.29 | −163.3 | −1.8 |
| | 4 | 10.43 | 168.5 | −20.8 |
| **J** | 1 | 0.00 | 0.0 | |
| | 2 | 1.95 | 180.0 | |
| **K** | 1 | 0.00 | 1.0 | |
| | 2 | 4.81 | 179.8 | |

[a] The torsion angle no. 1 is the central $\theta_{SCCS}$ angle for compound **B**, the $\theta_{CCCS}$ angle for compounds **C**, **D**, and **E**, and the $\theta_{C(0)CCC}$ angle for compounds **J** and **K**. [b]For compounds **C**, **D**, and **E**, torsion angle no. 2 is the central $\theta_{NCCC}$ angle.

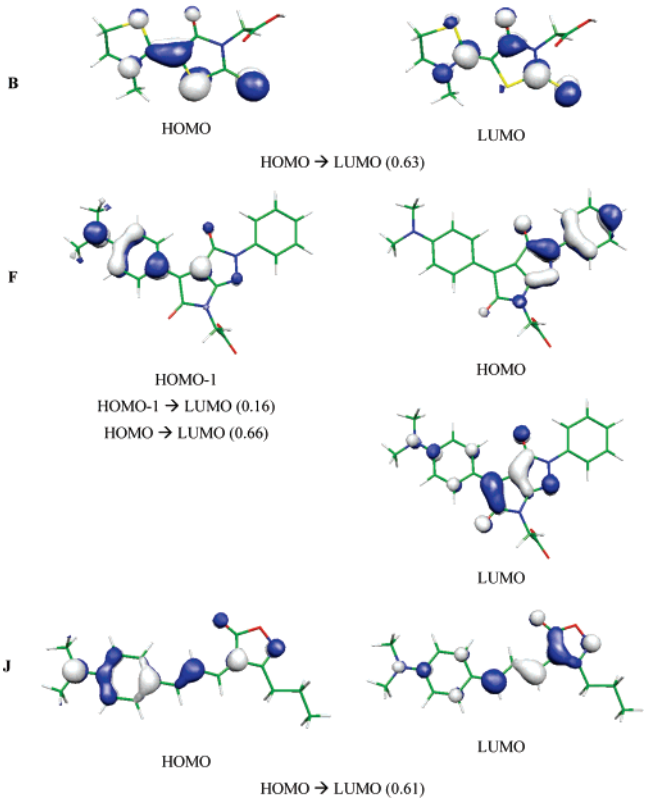


**Figure 1.** Sketch of the main molecular orbitals involved in the first dominant dipole-allowed transition for the **B**, **F**, and **J** compounds, obtained at the B3LYP/6-311G* level of approximation. Besides their label, the weights (normalized to $1/\sqrt{2}$) of the corresponding molecular orbitals in the excitation are given in parentheses.

of the $\Delta E$ variations between the different compounds. In the **A**−**E** family, the B3LYP/6-311G* theoretical estimates range between 2.63 (**C**) and 3.61 (**B**) eV while the experimental values, which are given in the same order, range between 2.20 and 3.15 eV (Table 3). For the compounds with a 2-thioxo 4-thiazolidinone group bearing nearly identical substituents on nitrogen ($CH_2-CH_3$ or $CH_2-COOH$) the $\Delta E$ ordering is more influenced by the conjugation length than by the donor strength of the other moiety. Compound **B** presents the shortest conjugation and the largest excitation energy. The conjugated path is the largest in compound **C** (smallest excitation energy), and then comes compound **E** where the S atom relays better the conjugation than the C atom in compound **D**. On the other hand, the donor strength was estimated from the sum of the Mulliken charges on the donor group. They amount to −0.054, −0.015, 0.287, 0.332, and 0.340 for the **C**, **A**, **D**, **E**, and **B** compounds, respectively. They do not exhibit clear relationships with the $\Delta E$ values. However, as discussed later, the systems presenting the smallest (negative) charges display the smallest solvatochromism. The excitation energies depend little on the conformation, at least when considering the most stable conformers described in the III-1 subsection. The largest effects are encountered for compound **B** where the variation of $\Delta E$ attains 0.10 eV, the smallest $\Delta E$ being associated with the less stable conformer. However, after accounting for Maxwell−Boltzmann weights, the impact is almost negligible.

**TABLE 2: Excitation Energies (and Corresponding Wavelengths) for the Dominant Low-Energy Absorption Band of Merocyanines Determined at the TDDFT Level of Approximation Using Different Exchange-Correlation Functionals and Basis Sets[a]**

| | B3LYP/6-311G* | | B3LYP/6-311+G* | | PBE0/6-311G* | |
|---|---|---|---|---|---|---|
| | $\Delta E$ (eV) | $\lambda$ (nm) | $\Delta E$ (eV) | $\lambda$ (nm) | $\Delta E$ (eV) | $\lambda$ (nm) |
| **A** | 3.19 | 389 | 3.12 | 397 | 3.26 | 380 |
| **B** | 3.61 | 343 | 3.56 | 348 | 3.70 | 335 |
| **C** | 2.63 | 471 | 2.60 | 477 | 2.72 | 456 |
| **D** | 2.98 | 416 | 2.92 | 425 | 3.05 | 407 |
| **E** | 2.84 | 437 | 2.81 | 441 | 2.91 | 426 |
| **F** | 2.67 | 464 | 2.63 | 472 | 2.75 | 453 |
| **G** | 2.61 | 476 | 2.56 | 484 | 2.67 | 465 |
| **H** | 2.59 | 478 | 2.54 | 488 | 2.65 | 467 |
| **I** | 2.65 | 467 | 2.61 | 475 | 2.72 | 456 |
| **J** | 2.90 | 427 | 2.86 | 433 | 2.97 | 418 |
| **K** | 3.27 | 379 | 3.24 | 383 | 3.34 | 371 |

[a] Maxwell−Boltzmann averaging for $T = 298.15$ K is performed when several conformers present similar energies.

The range of $\Delta E$ variation is much smaller for the **F**−**I** group. However, one can notice a small decrease of $\Delta E$ with the strength of the donor group, that is, with the size of the N substituents. Then, consistently with the experiment, the calculations report a small decrease in $\Delta E$ associated with the presence of the COOH acceptor, as observed when comparing compounds **F** and **I**. Then, for **J** and **K**, which differ by the substituent on the phenyl ring and the length of the polyenic segment, the smallest $\Delta E$ is associated with the longest conjugated linker. This analysis of the three types of merocyanines shows that theory nicely reproduces the trends in $\Delta E$ upon chemical modifications of the chromophores. As expected from recent literature, the TDDFT values are overestimated: at the B3LYP/6-311G* level, the differences range from 0.40 eV (17.6%) for molecule **F** to 0.58 eV (26%) for molecule **I** with respect to the experimental data recorded in methanol solutions. Then, the variations of these differences with the basis set and the exchange-correlation functional are too small with respect to the gap between the calculated and experimental values (Table 3), showing the necessity to improve the simulations by accounting first for the effects of the solvent.

**III-4. Modeling the Solvent Effects.** Thus, as a natural follow-up, the solvent effects were modeled. Using the IEFPCM scheme, three solvents were considered: methanol, acetonitrile, and dimethyl sulfoxide (DMSO) in increasing order of polarity (in the same order, their dielectric constant amounts to 32.63,

**TABLE 3: Theoretical and Experimental Excitation Energies of Merocyanines Corresponding to the Main Low-Energy Charge Transfer Excited States**[a]

| | theory | | | | experiment |
|---|---|---|---|---|---|
| | vacuo | methanol | acetonitrile | DMSO | $\Delta E$ (eV) |
| **A** | 3.19 (18.1%) | 3.07 (13.7%) | 3.06 (13.3%) | 3.03 (12.2%) | 2.70 |
| **B** | 3.61 (14.6%) | 3.45 (9.5%) | 3.44 (9.2%) | 3.42 (8.6%) | 3.15 |
| **C** | 2.63 (19.5%) | 2.58 (17.3%) | 2.58 (17.3%) | 2.54 (15.5%) | 2.20 |
| **D** | 2.98 (20.6%) | 2.70 (9.3%) | 2.70 (9.3%) | 2.67 (8.1%) | 2.47 |
| **E** | 2.84 (20.3%) | 2.65 (12.3%) | 2.64 (11.9%) | 2.61 (10.6%) | 2.36 |
| **F** | 2.67 (17.6%) | 2.46 (8.4%) | 2.46 (8.4%) | 2.43 (7.0%) | 2.27 |
| **G** | 2.61 (20.3%) | 2.41 (11.1%) | 2.41 (11.1%) | 2.38 (9.7%) | 2.17 |
| **H** | 2.59 (19.9%) | 2.40 (11.1%) | 2.40 (11.1%) | 2.37 (9.7%) | 2.16 |
| **I** | 2.65 (18.8%) | 2.45 (9.9%) | 2.45 (9.9%) | 2.42 (8.5%) | 2.23 |
| **J** | 2.90 (23.9%) | 2.65 (13.3%) | 2.64 (12.8%) | 2.60 (11.1%) | 2.34 |
| **K** | 3.27 (17.6%) | 3.10 (11.5%) | 3.09 (11.2%) | 3.06 (10.1%) | 2.78 |

[a] The theoretical values were obtained using the TDDFT/B3LYP/6-311G* method and the IEFPCM scheme. The experimental values were obtained in methanol solutions and correspond to the absorption maximum. The values in parentheses indicate the relative error with respect to the experimental value. Maxwell−Boltzmann averaging for $T = 298.15$ K is performed when several conformers present similar energies.

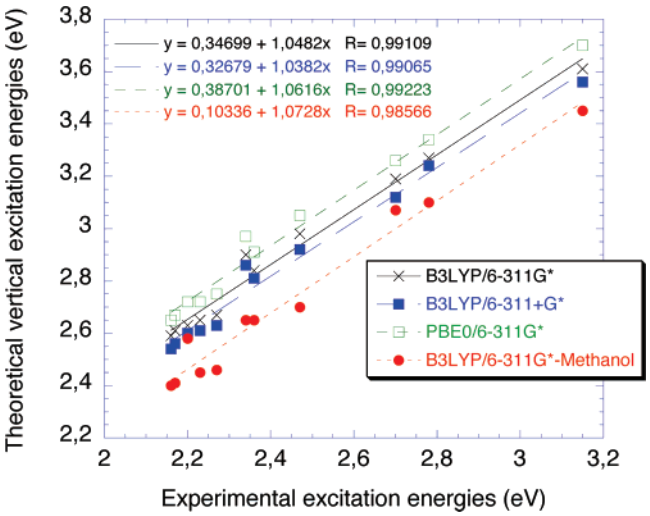


**Figure 2.** Theoretical versus experimental excitation energies of merocyanine dyes for different levels of approximation.

36.64, and 46.7, respectively). The results reported in Table 3 show a significant reduction in $\Delta E$, up to 0.31 eV, when accounting for the solvent effects, whereas the differences between methanol, acetonitrile, and DMSO are mostly negligible. In fact, the $\Delta E$ variations between the different solvents are of the same order of magnitude as the effects of the exchange-correlation functional and basis set described above.

Comparing now the IEFPCM results for methanol with the experimental ones, it appears that the overestimation of the excitation energies is corrected partially when the solvent effects are included. The remaining deviation ranges now from 8.4% for molecule **F** to 17.3% for molecule **C**. From a comparison with DMSO calculated data, these remaining errors are not related to the solvent polarity, at least as taken into account with the IEFPCM scheme.

**III-5. Linear Fits.** The relationships between theory and experiment have been further scrutinized by performing linear regressions (Figure 2). The correlation coefficients are all larger than 0.98, demonstrating, as already discussed, qualitatively for the different types of merocyanines, the good behavior of the TDDFT scheme. The values of the ordinates at the origin account for the systematic overestimations of the excitation energies with TDDFT and their substantial decreases (58%) when including the effects of the solvent. On the other hand, the exchange-correlation functional and the basis set have only a small impact on the ordinates at the origin. The slopes are slightly larger than 1, which corresponds to a small overestimation of the variations of the excitation energies by the TDDFT method. By employing these linear regressions, expressions to estimate the experimental excitation energies from the theoretical ones have been deduced (in eV):

$$\Delta E(\text{exp.}) = -0.3310 + 0.9540 \times \Delta E(\text{B3LYP/6-311G*}) \quad (1)$$

$$\Delta E(\text{exp.}) = -0.0963 + 0.9321 \times \Delta E(\text{B3LYP/6-311G*/IEFPCM-methanol}) \quad (2)$$

Applying these two equations leads to remaining deviations ranging from −0.05 to 0.09 eV for the first equation and from −0.07 to 0.06 eV for the IEFPCM equation, a precision that allows the estimation, with a rather good accuracy, of the absorption maximum wavelength of new merocyanine dyes from rapid TDDFT calculations. These experiment−theory relationships can be compared with those determined recently in a similar study on cyanines:[50]

$$\Delta E(\text{exp.}) = -0.9684 + 1.1827 \times \Delta E(\text{B3LYP/6-311G*}) \quad (3)$$

$$\Delta E(\text{exp.}) = -0.6017 + 1.0941 \times \Delta E(\text{B3LYP/6-311G*/IEFPCM-methanol}) \quad (4)$$

Although the same trends are observed, that is, the ordinate at the origin is substantially reduced and the slope gets closer to 1 when including solvent effects, there are quantitative differences, in particular, in what concerns the ordinate at the origin, which is about 0.5−0.6 eV larger in the case of the cyanines. The slopes also differ, though by only 16−23%. This comparison demonstrates that the experiment−theory relationships based on TDDFT calculations depend on the nature of the compounds and that their use should be restricted to families of similar compounds, or as shown by Grimme and Parac, to families of similar excitations.[25] This further demonstrates that, using conventional exchange-correlation functionals and the adiabatic approximation, the systematic errors depend on the chemical nature of the systems.

**III-6. Vibrational Structures.** The above analysis shows the two kinds of errors that are made when calculating the excitation energies, (i) systematic errors, which can be partially corrected using linear scaling procedures, and (ii) nonsystematic errors having different origins. The latter are due to the inherent approximations of the exchange-correlation functionals and the lack of treatment of vibronic effects. Indeed, reported experimental excitation energies correspond to absorption maxima, taking implicitly into account the geometry relaxations in the

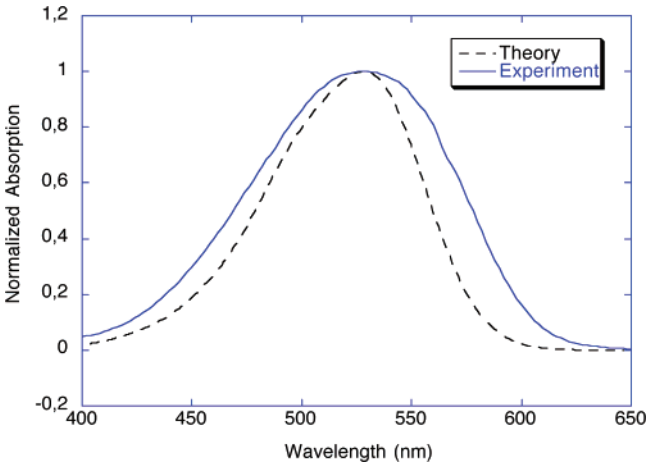


**Figure 3.** Theoretical and experimental absorption spectra of the **J** compound as determined at BHandHLYP/SV(P) level of approximation. The vibrational structure has been obtained after convoluting the Franck−Condon factors with Gaussian functions having a full width at half-magnitude of 0.2 eV. The theoretical spectrum has been shifted by 0.67 eV so that the two maximum absorption energies coincide.

excited state and the vibrational structure, while the theoretical values are merely vertical electronic excitation energies. These effects have been studied for the molecule **J** using the BHandHLYP exchange-correlation functional. At this level of approximation, the (vertical) $\Delta E$ value amounts to 3.35 eV, whereas the gap between the ground vibrational states of the electronic ground and excited states, $E_{0-0}$, amounts to 2.95 eV. Then, when accounting for the vibrational structures, as shown in Figure 3, the maximum absorption is located at an excitation energy of 3.02 eV. Thus, the vibronic effects account for a red shift of $\Delta E$ by 0.33 eV. Assuming that the vibronic and solvent effects are additive, we determine the new theoretical estimate to be 2.65 − 0.33 eV = 2.32 eV in comparison with the 2.34 eV experimental value.

## IV. Conclusions and Outlook

The visible spectral properties of a set of merocyanine dyes have been determined experimentally and compared to theoretical estimates calculated at different levels of approximation using TDDFT. In the first family, the merocyanines contain the 4-thiazolidinone, 2-thioxo group in resonance with different donor groups. The merocyanines of the second family present a common pyrrolo[2,3-*c*]pyrazole-6-(2*H*)-acetic acid, 4-[4-(dialkylamino)phenyl]-3,5-dihydro-3,5-dioxo-2-phenyl group with different substituents on the two phenyl rings. Two compounds form the last family. They are constituted of an isoxazolone group linked via a conjugated polyenic segment to an aminophenyl group bearing different substituents.

Two hybrid exchange-correlation functionals have been used, whereas solvent effects have been included using the IEFPCM. Moreover, the vibrational structure of the electronic transitions has been determined by calculating the Franck−Condon factors within the Born−Oppenheimer approximation, whereas the impact of the presence of several conformers at room temperature has been accounted for by using the Maxwell−Boltzmann distribution scheme.

The TDDFT calculations show that the dominant transitions have a $\pi-\pi^*$ character. They reproduce nicely the variations of excitation energies with the nature of the merocyanine so that least-squares fits can be used to correct for the major systematic errors of the computational scheme and therefore to reach an accuracy of 0.09 eV or better. Part of these systematic errors is shown to originate from the description of the solvent, whereas vibronic effects can account for most of the remaining differences.

**Acknowledgment.** This work is supported by the "Institute for the Promotion of Innovation by Science and Technology in Flanders (IWT)". B.C. thanks the FNRS for his Research Director position. The calculations have been performed on the Interuniversity Scientific Computing Facility (ISCF), installed at the Facultés Universitaires Notre-Dame de la Paix (Namur, Belgium), for which the authors gratefully acknowledge the financial support of the FNRS-FRFC and the "Loterie Nationale" for the convention no. 2.4578.02, and of the FUNDP.

## References and Notes

(1) Zuppiroli, L.; Bussac, M. N. *Traité des Couleurs*; Presses Polytechniques et Universitaires Romandes: Lausanne, 2001.
(2) Argun, A. A.; Aubert, P. H.; Thompson, B. C.; Schwendeman, I.; Gaupp, C. L.; Hwang, J.; Pinto, N. J.; Tanner, D. B.; MacDiarmid, A. G.; Reynolds, J. R. *Chem. Mater.* **2004**, *16*, 4401−4412.
(3) Sanguinet, L.; Pozzo, J. L.; Rodriguez, V.; Adamietz, F.; Castet, F.; Ducasse, L.; Champagne, B. *J. Phys. Chem. B* **2005**, *109*, 11139−11150.
(4) Raymo, F. M.; Tomasulo, M. *Chem.—Eur. J.* **2006**, *12*, 3186−3193.
(5) Albert, I. D. L.; Marks, T. J.; Ratner, M. A. *J. Phys. Chem.* **1996**, *100*, 9714−9725.
(6) Champagne, B.; Legrand, T.; Perpète, E. A.; Quinet, O.; André, J. M. *Collect.* Czech. Chem. Commun. **1998**, *63*, 1295−1308.
(7) Sainudeen, Z.; Ray, P. C. *J. Phys. Chem. A* **2005**, *109*, 9095−9103.
(8) Reichardt, C. *Chem. Rev.* **1994**, *94*, 2319−2358.
(9) Baraldi, I.; Momicchioli, F.; Ponterini, G.; Vanossi, D. *Chem. Phys.* **1998**, *238*, 353−364.
(10) Baraldi, I.; Brancolini, G.; Momicchioli, F.; Ponterini, G.; Vanossi, D. *Chem. Phys.* **2003**, *288*, 309−325.
(11) Abdel-Halim, S. T.; Awad, M. K. *J. Chem. Phys.* **1993**, *97*, 3160−3165.
(12) Abdel-Halim, S. T.; Awad, M. K. *J. Mol. Struct.* **2005**, *754*, 16−24.
(13) Hammam, E.; El-Nahas, A. M. *J. Phys. Chem. A* **1998**, *102*, 9739−9744.
(14) Millié, P.; Momichhioli, F.; Vanossi, D. *J. Phys. Chem. B* **2000**, *104*, 9621−9629.
(15) Mach, P.; Urban, J.; Leszczynski, J. *Int. J. Quantum Chem.* **2002**, *87*, 265−269.
(16) Liu, T.; Han, W.-E.; Himo, F.; Ullmann, G. M.; Bashford, D.; Touchkine, A.; Hahn, K. M.; Noodleman, L. *J. Chem. Phys.* **2004**, *108*, 3545−3555.
(17) Runge, E.; Gross, E. K. U. *Phys. Rev. Lett.* **1984**, *52*, 997−1000.
(18) Bauernschmitt, R.; Ahlrichs, R. *Chem. Phys. Lett.* **1996**, *256*, 454−464.
(19) Casida, M. E.; Jamorski, C.; Casida, K. C.; Salahub, D. R. *J. Chem. Phys.* **1998**, *108*, 4439−4449.
(20) Tozer, D. J.; Handy, N. C. *J. Chem. Phys.* **1998**, *109*, 10180−10189.
(21) Sundholm, D. *Chem. Phys. Lett.* **1999**, *302*, 480−484.
(22) Schipper, P. R. T.; Gritsenko, O. V.; van Gisbergen, S. J. A.; Baerends, E. J. *J. Chem. Phys.* **2000**, *112*, 1344−1356.
(23) Full, J.; González, L.; Daniel, C. *J. Phys. Chem. A* **2001**, *105*, 184−189.
(24) Cavillot, V.; Champagne, B. *Chem. Phys. Lett.* **2002**, *354*, 449−457.
(25) Parac, M.; Grimme, S. *Chem. Phys.* **2003**, *292*, 11−21.
(26) Jamorski-Jödicke, C.; Lüthi, H. P. *J. Am. Chem. Soc.* **2003**, *125*, 252−264.
(27) Rappoport, D.; Furche, F. *J. Am. Chem. Soc.* **2004**, *126*, 1277−1284.
(28) Masunov, A.; Tretiak, S. *J. Phys. Chem. B* **2004**, *108*, 899−907.
(29) Grozema, F. C.; van Duijnen, P. T.; Siebbeles, L. D. A.; Goossens, A.; de Leeuw, S. W. *J. Phys. Chem. B* **2004**, *108*, 16139−16146.
(30) Blanco Rodriguez, A. M.; Gabrielsson, A.; Motevalli, M.; Matousek, P.; Towrie, M.; Sebera, J.; Zalis, S.; Vlcek, A., Jr. *J. Phys. Chem. A* **2005**, *109*, 5016−5025.
(31) Jacquemin, D.; Préat, J.; Wathelet, V.; André, J. M.; Perpète, E. *Chem. Phys. Lett.* **2005**, *405*, 429−433.
(32) Homem-de-Mello, P.; Mennucci, B.; Tomasi, J.; da Silva, A. B. F. *Theor. Chem. Acc.* **2005**, *113*, 274−280.
(33) Sekino, H.; Bartlett, R. J. *Int. J. Quantum Chem.* **1984**, *S18*, 255−263.

(34) Andersson, K.; Malmqvist, P. A.; Roos, B. O.; Sadlej, A. J.; Wolinski, K. *J. Phys. Chem.* **1990**, *94*, 5483−5488.
(35) Grimme, S.; Parac, M. *ChemPhysChem* **2003**, *3*, 292−295.
(36) Dreuw, A.; Weisman, J. L.; Head-Gordon, M. *J. Chem. Phys.* **2003**, *119*, 2943−2946.
(37) Tawada, Y.; Tsuneda, T.; Yanagisawa, S.; Yanai, T.; Hirao, K. *J. Chem. Phys.* **2004**, *120*, 8425−8433.
(38) Peach, M. J. G.; Helgaker, T.; Salek, P.; Keal, T. W.; Lutnæs, O. B.; Tozer, D. J.; Handy, N. C. *Phys. Chem. Chem. Phys.* **2006**, *8*, 558−562.
(39) Chiba, M.; Tsuneda, T.; Hirao, K. *J. Chem. Phys.* **2006**, *124*, 144106.
(40) d'Antuono, P.; Botek, E.; Champagne, B.; Wieme, J.; Reyniers, M. F.; Marin, G. B.; Adriaensens, P. J.; Gelan, J. *Chem. Phys. Lett.* **2005**, *411*, 207−213.
(41) Tomasi, J.; Mennucci, B.; Cammi, R. *Chem. Rev.* **2005**, *105*, 2999−3094.
(42) Mennucci, B.; Cammi, R.; Tomasi, J. *J. Chem. Phys.* **1998**, *109*, 2798−2807.
(43) Frisch, M. J.; Trucks, G. W.; Schlegel, H. B.; Scuseria, G. E.; Robb, M. A.; Cheeseman, J. R.; Montgomery, J. A., Jr.; Vreven, T.; Kudin, K. N.; Burant, J. C.; Millam, J. M.; Iyengar, S. S.; Tomasi, J.; Barone, V.; Mennucci, B.; Cossi, M.; Scalmani, G.; Rega, N.; Petersson, G. A.; Nakatsuji, H.; Hada, M.; Ehara, M.; Toyota, K.; Fukuda, R.; Hasegawa, J.; Ishida, M.; Nakajima, T.; Honda, Y.; Kitao, O.; Nakai, H.; Klene, M.; Li, X.; Knox, J. E.; Hratchian, H. P.; Cross, J. B.; Bakken, V.; Adamo, C.; Jaramillo, J.; Gomperts, R.; Stratmann, R. E.; Yazyev, O.; Austin, A. J.; Cammi, R.; Pomelli, C.; Ochterski, J. W.; Ayala, P. Y.; Morokuma, K.; Voth, G. A.; Salvador, P.; Dannenberg, J. J.; Zakrzewski, V. G.; Dapprich, S.; Daniels, A. D.; Strain, M. C.; Farkas, O.; Malick, D. K.; Rabuck, A. D.; Raghavachari, K.; Foresman, J. B.; Ortiz, J. V.; Cui, Q.; Baboul, A. G.; Clifford, S.; Cioslowski, J.; Stefanov, B. B.; Liu, G.; Liashenko, A.; Piskorz, P.; Komaromi, I.; Martin, R. L.; Fox, D. J.; Keith, T.; Al-Laham, M. A.; Peng, C. Y.; Nanayakkara, A.; Challacombe, M.; Gill, P. M. W.; Johnson, B.; Chen, W.; Wong, M. W.; Gonzalez, C.; Pople, J. A. *Gaussian 03*, revision C.02; Gaussian, Inc.: Wallingford, CT, 2004.
(44) Kallies, B. *TURBOMOLE*: *Program Package for ab initio Electronic Structure Calculations*, version 5.6; University of Karlsruhe: Karlsruhe, Germany, 2004.
(45) Deglmann, P.; Furche, F.; Ahlrichs, R. *Chem. Phys. Lett.* **2002**, *362*, 511−518.
(46) Dierksen, M.; Grimme, S. *J. Phys. Chem. A* **2004**, *108*, 10225−10237.
(47) Doktorov, E. V.; Malkin, I. A.; Man'ko, V. I. *J.* Mol. Spectrosc. **1997**, *64*, 302−326.
(48) Spangenberg, D.; Imhof, P.; Kleinermanns, K. *Phys. Chem. Chem. Phys.* **2003**, *5*, 2505−2514.
(49) Sanguinet, L.; Pozzo, J. L.; Guillaume, M.; Champagne, B.; Castet, F.; Ducasse, L.; Maury, E.; Soulié, J.; Mançois, F.; Adamietz, F.; Rodriguez, V. *J. Phys. Chem. B* **2006**, *110*, 10672−10682.
(50) Champagne, B.; Guillaume, M.; Zutterman, F. *Chem. Phys. Lett.* **2006**, *425*, 105−109.